PHOTON NUMBER AMPLIFICATION/DUPLICATION THROUGH PARAMETRIC CONVERSION

G. M. D'Ariano, C. Macchiavello, and M. Paris

Dipartimento di Fisica 'Alessandro Volta', via Bassi 6, I-27100 Pavia, Italy

ABSTRACT: The performance of parametric conversion in achieving number amplification and duplication is analyzed. It is shown that the effective maximum gains G_* remain well below their integer ideal values, even for large signals. Correspondingly one has output Fano factors F_* which are increasing functions of the input photon number. In the inverse (deamplifier/recombiner) operating mode, on the contrary, quasi ideal gains G_* and small factors $F_* \simeq 10\%$ are obtained. Output noise and nonideal gains are ascribed to spontaneous parametric emission.

1. INTRODUCTION

The ultimate transparency of optical networks is essentially quantum-limited and any improvement beyond the standard performance depends on availability of nonstandard high quality quantum amplifiers. The *photon number amplifier* (PNA) and the *photon number duplicator* (PND) are the quantum devices which are needed in direct detection.[1] The PNA ideally should affect the state transformation

$$|n\rangle \longrightarrow |Gn\rangle \tag{1}$$

for integer gains G and input eigenstates $|n\rangle$ of the number. Similarly, the PND, instead of amplifying the photon number, produces two copies of the same input state for eigenstates of the number, namely

$$|n\rangle \longrightarrow |n,n\rangle\ . \tag{2}$$

Both devices are particularly suited to local area network environments, where the minimum loss for user-derivation is 3dB (in average), and transparency rapidly degrades with the increasing number of users. In such situation the PNA represents the ideal preamplifier to be inserted before each derivation, whereas the PND—which ideally realizes the quantum nondemolition measurement of the number—could itself be used as an ideal lossless optical tap.

The PNA and PND could also be profitably used in the inverse operating mode, namely the PNA as a *number deamplifier* and the PND as a *number recombiner*. The number deamplifier could be used as a *number squeezer*, allowing production of subpoissonian states from coherent light; the

number recombiner, on the other hand, could produce novel nonclassical radiation from input twin-beams [an example of such application in production of phase-coherent states[2] is proposed in Ref. [3]].

The concrete realization of high quality PNA and PND for practical applications is an arduous task. As explained in Ref. [4], number conversion, in a way similar to the customary conversion, requires a medium with a $\chi^{(2)}$ or $\chi^{(3)}$ susceptibility, but here with a phase-dependent polarizability. More precisely, almost ideal number conversion can be achieved upon modulating the nonlinear susceptibility at a $(G-1)$-submultiple of the wavelenght of the amplified mode, G being the integer gain [feasibility studies of number conversion using multiple quantum wells heterostructures are currently in progress[6]]. The required phase-dependent polarizability in a $\chi^{(2)}$ or $\chi^{(3)}$ medium may also be regarded as an intensity-dependent coupling for a $\chi^{(G)}$ or $\chi^{(G+1)}$ medium (simply from polar decomposition of the boson field operators). This suggests that a gain-two PNA should be simpler to realize than a generic $G > 2$ amplifier. However, as also explained in this paper, the intensity dependent coupling should follow the power low $(a^\dagger a+1)^{-1/2}$, $a^\dagger a$ being the number operator of the amplified mode. Such a decreasing factor is essentially the $(1+I)^{-1/2}$ saturating behaviour of a two level system effective susceptibility in the inhomogeneous-broadening limit,[5] but it is not obvious that this power low—which is obtained in a semiclassical context—could survive in the quantization procedure.

The previous observations quite naturally lead to ask if the conventional conversion could somehow simulate the number conversion, and what would be the range of physical parameters where ideal behaviour is better approximated: this is the subject of the present paper. Quite unexpectedly (see for example Ref. [1]) we find that ideal behaviour is never approached, even in the limit of large input signals. The most striking result is that conversion is never complete and, therefore, the effective maximum gains G_∞ remain well below their integer ideal values, even for large input photon numbers: quantum mechanics thus reveals its subtle nature even for large quantum numbers, here in form of noise in amplifiers [for a discussion on applicability of the correspondence principle in a different context, see Ref. [7]].

The inverse devices—namely the number deamplifier and the number recombiner—are better approximated by parametric conversion than the direct ones. We will show that ideal gains are achieved in the large-n limit, whereas Fano factors F_∞ remain nonvanishing but small ($F_\infty \simeq 10\%$). Therefore, it seems that at present the devices which are simplest to realize concretely should be the number deamplifier and the number recombiner (even though probably the limited output noise of the deamplifier could not be satisfactory for applications as number squeezer).

After presenting the theory of the ideal devices in Sect.2, the connections between the conventional and the number conversions are explained in Sect.3, where a simple mean field approach for analytical evaluation of the conversion time is also given. In Sect.4 the announced numerical results on conversion times, effective gains and Fano factors are presented. In Sect.5 we conclude with some remarks on the physical interpretation of the nonideal behaviour in terms of spontaneous parametric emission.

2. THE IDEAL NUMBER AMPLIFIER/DUPLICATOR

In the Heisenberg picture the ideal PNA corresponds to multiplication of the number operator by the integer gain G

$$a^\dagger a \to G a^\dagger a\,, \tag{3}$$

a being the annihilator of the amplified mode of the field. Because of the integer nature of $a^\dagger a$,

the deamplifier does not trivially correspond to replace G into G^{-1} in Eq. (3). Actually the ideal deamplification is the following

$$a^\dagger a \to [G^{-1}a^\dagger a] \,, \tag{4}$$

where $[x]$ denotes the integer part of x. As a consequence, even in the ideal case, the deamplification has an input-dependent effective gain $G_.$

$$G_. = \frac{[G^{-1}n]}{n} \leq G^{-1} \tag{5}$$

for n input photons, and $G_. \simeq G^{-1}$ for large n. [As an example, the case $G = 2$ is depicted in Fig. 4.] In terms of the shift operator $\hat{e}_+ : \hat{e}_+|n\rangle = |n+1\rangle$, the transformation (4) is obtained as follows

$$\hat{e}_+ \to (\hat{e}_+)^G \,, \tag{6}$$

where now $(\hat{e}_+)^G|n\rangle = |n+G\rangle$. In fact, the map (6) corresponds to the following[3]

$$a^\dagger \to a^\dagger_{(G)} \,, \tag{7}$$

where $a^\dagger_{(G)}$ is a boson operator creating G photons at a time,[8] namely

$$a^\dagger_{(G)}|n\rangle = \sqrt{[G^{-1}n]+1}\,|n+G\rangle \,, \tag{8}$$

$$\left[a_{(G)}, a^\dagger_{(G)}\right] = 1 \,, \quad \left[a_{(G)}, a^\dagger a\right] = G a_{(G)} \,. \tag{9}$$

The explicit form of $a^\dagger_{(G)}$ is

$$a^\dagger_{(G)} = \left\{\frac{[G^{-1}\hat{n}](\hat{n}-G)!}{\hat{n}!}\right\}^{1/2} (a^\dagger)^G \tag{10}$$

and from Eq. (10) it follows that

$$a^\dagger_{(G)} a_{(G)} = [G^{-1}a^\dagger a] \,, \tag{11}$$

which is the deamplification (4). The direct amplification (3) corresponds to the inverse transformation

$$a^\dagger_{(G)} \to a^\dagger \tag{12}$$

[see Ref. [3] for more details about these maps]. The transformations (7) and (12) are essentially permutations of two different types of boson. For commuting modes $[a, c] = [a, c^\dagger] = 0$ the permuting map $a \leftrightarrow c$ is realized by the Heisenberg evolution

$$PaP = c, \qquad PcP = a \,, \tag{13}$$

where

$$P = P^\dagger = \exp\left(i\frac{\pi}{2}c^\dagger c\right) \exp\left[-i\frac{\pi}{2}\left(a^\dagger c + c^\dagger a\right)\right] \exp\left(i\frac{\pi}{2}c^\dagger c\right) \,. \tag{14}$$

However, as a and $a_{(G)}$ do not commute, it is convenient to consider a simultaneous change of the field mode (namely the amplifier also converts the frequency or changes the field polarization). In this case the amplifying operator is

$$P_{(G)} = \exp\left(i\frac{\pi}{2}c^\dagger c\right)\exp\left[-i\frac{\pi}{2}\left(a^\dagger_{(G)}c + c^\dagger a_{(G)}\right)\right]\exp\left(i\frac{\pi}{2}c^\dagger c\right) . \tag{15}$$

The operator (15) now attains the transformations

$$P_{(G)}(\hat{1}\otimes\hat{e}_+)P_{(G)} = (\hat{e}_+)^G\otimes\hat{1} , \qquad P_{(G)}\left[(\hat{e}_+)^G\otimes\hat{1}\right]P_{(G)} = \hat{1}\otimes\hat{e}_+ , \tag{16}$$

where in the tensor notation $\hat{O}_1\otimes\hat{O}_2$ the first entry is for the a mode and the second entry for the c mode. The Schrödinger evolutions of the number eigenstates corresponding to the amplifying and deamplifying operating modes are

$$P_{(G)}|0,n\rangle = |Gn,0\rangle , \tag{17}$$

$$P_{(G)}|n,0\rangle = |G\langle G^{-1}n\rangle, [G^{-1}n]\rangle , \tag{18}$$

where $\langle x\rangle = x - [x]$ denotes the fractional part of x and $|n,m\rangle = |n\rangle_a\otimes|m\rangle_c$. If one would consider only one mode in the above transformations—say a—a frequency conversion $P_{(1)}$ is needed. In this case the evolutions (17-18) rewrite

$$P_{(G)}P_{(1)}|n,0\rangle = |Gn,0\rangle \tag{19}$$

$$P_{(1)}P_{(G)}|0,n\rangle = |G\langle G^{-1}n\rangle, [G^{-1}n]\rangle , \tag{20}$$

whereas totally ignoring the mode c corresponds to trace the transformations (19-20) over this mode, adopting a density matrix representation for states. In this way nonunitary transformations for the reduced density matrix of the signal mode a are obtained, which do not preserve the Newmann-Shannon entropy: these are the 'photon fractioning' and 'multiphoton' transformations of Refs.[3,9]. The mode c is responsible of the added noise which is present even in the ideal case (see Eq. (5)) and corresponds to the 'idler mode' of the customary linear amplification.[3]

Apart from the $\frac{\pi}{2}$ phase shift—which can be obtained by changing the optical path of the b mode and which, however, for an input number eigenstate corresponds to an irrelevant overall phase factor—the evolution operator (15) comes from the interaction Hamiltonian in the Dirac picture

$$\hat{H}_I = a^\dagger_{(G)}c + \text{h.c.} \tag{21}$$

for a dimensionless evolution time

$$\tau_* = \frac{\pi}{2} . \tag{22}$$

The Hamiltonian (21) has the following constants of motion

$$\hat{s}_A = a^\dagger a + Gc^\dagger c , \tag{23}$$

$$\hat{d}_A = G\langle G^{-1}a^\dagger a\rangle = G\langle G^{-1}\hat{s}_A\rangle , \tag{24}$$

and, because of identity (24), only $\hat{s}_A$ must be specified. In the following evaluations we use the basis of the Hilbert subspace corresponding to fixed $\hat{s}_A$ eigenvalues

$$|n\rangle_{s_A} = |s_A - Gn, n\rangle , \qquad n = 0,1,\ldots[G^{-1}s_A] \tag{25}$$

In this basis Eqs. (17-18) rewrite

$$P_{(G)}|n\rangle_{Gn} = |0\rangle_{Gn} \,, \tag{26}$$

$$P_{(G)}|0\rangle_n = |[G^{-1}n]\rangle_n \,, \tag{27}$$

whereas the Hamiltonian (21) takes the tridiagonal form

$$\hat{H}_I|n\rangle_s = \alpha_n^{(s)}|n-1\rangle_s + \alpha_{n+1}^{(s)}|n+1\rangle_s \,, \tag{28}$$

$$\alpha_n^{(s)} = \sqrt{n([G^{-1}s] - n + 1)} \,. \tag{29}$$

Conservation of the interaction Hamiltonian (21) itself corresponds to the resonance condition $G\omega_a = \omega_c$. In the nonresonating case a third pump mode d is needed with $\omega_d = G\omega_a - \omega_c$: Eq. (21) is obtained from the interaction Hamiltonian in the Schrödinger picture

$$\hat{H}' = a_{(G)}^{\dagger} cd + \text{h.c.} \tag{30}$$

in the parametric approximation of classical undepleted pump, namely with d in a highly excited coherent state.

The photon number duplicator in some respect is similar to the gain-2 photon number amplifier. Instead of amplifying the number of photons, it produces two copies of the same input state for eigenstates of the number operator. If the input copies are carried by the modes a and b whereas the output by c, the duplication map reads

$$|0,0,n\rangle \rightarrow |n,n,0\rangle \tag{31}$$

and is trivially inverted for $n_a = n_b$ [for the general case see Ref. [3]]. The state transformation (31) corresponds to the Heisenberg evolution

$$\hat{e}_+ \otimes \hat{e}_+ \otimes \hat{1} \rightarrow \hat{1} \otimes \hat{1} \otimes \hat{e}_+ \,, \tag{32}$$

which is obtained as permutation of the boson operators $a_{(1,1)}$ and c, where $a_{(1,1)}^{\dagger}$ now denotes the two-mode creator

$$a_{(1,1)}^{\dagger}|n_a,n_b\rangle = \sqrt{(\min\{n_a,n_b\})+1}\,|n_a+1,n_b+1\rangle \,, \tag{33}$$

$$[a_{(1,1)}, a_{(1,1)}^{\dagger}] = 1 \,, \qquad [a_{(1,1)}, a^{\dagger}a + b^{\dagger}b] = 2a_{(1,1)} \,. \tag{34}$$

The following realization of $a_{(1,1)}^{\dagger}$ is obtained in Ref. [3]

$$a_{(1,1)}^{\dagger} = a^{\dagger}b^{\dagger}\frac{1}{\sqrt{\max\{a^{\dagger}a, b^{\dagger}b\}+1}} \,. \tag{35}$$

In a way analogous to the PNA, the Dirac picture interaction Hamiltonian of the PND is

$$\hat{H}_I = a_{(1,1)}^{\dagger} c + \text{h.c.} \,, \tag{36}$$

with constants of motion

$$\hat{s}_D = \frac{1}{2}\left(a^{\dagger}a + b^{\dagger}b + 2c^{\dagger}c\right) \,, \tag{37}$$

$$\hat{d}_D = a^{\dagger}a - b^{\dagger}b \,. \tag{38}$$

The Hilbert subspace of interest for duplication corresponds to $d_D = 0$; the subspaces for fixed eigenvalues s_D are spanned by the eigenvectors

$$|n\rangle_{s_D} = |s_D - n, s_D - n, n\rangle \,. \tag{39}$$

For fixed s_D the Hamiltonian (36) has the tridiagonal form

$$\hat{H}_I|n_s\rangle = \beta_n^{(s)}|n\ -1\rangle_s + \beta_{n+1}^{(s)}|n+1\rangle_s \,, \tag{40}$$

$$\beta_n^{(s)} = \sqrt{(s-n+1)n} \,. \tag{41}$$

Frequency conversion and simultaneous duplication require a classical undepleted pump mode d at frequency $\omega_d = \omega_a + \omega_b - \omega_c$, with interaction Hamiltonian

$$\hat{H}' = a_{(1,1)}^\dagger cd + \text{h.c.} \tag{42}$$

3. NUMBER-OPTIMIZED DOWNCONVERSION

The Hamiltonians (30) and (42) are complicated by the occurrence of the multiboson operators $a_{(G)}^\dagger$ and $a_{(1,1)}^\dagger$. An outlook at Eqs. (10) and (33) reveals that the G-photon amplification corresponds to a $\chi^{(G+1)}$ susceptibility and the duplication to a $\chi^{(3)}$. In the followings the $G = 2$ case—the simplest to attain in practice—will be considered only. For $\langle a^\dagger a\rangle \gg 2$ the two photon operator $a_{(2)}^\dagger$ can be approximated as follows

$$a_{(2)}^\dagger \simeq a^{\dagger 2}\left[2(a^\dagger a+1)\right]^{-\frac{1}{2}} \,, \qquad (\langle a^\dagger a\rangle \gg 2) \,. \tag{43}$$

On the other hand, for $d_D = 0$ the two-mode operator $a_{(1,1)}^\dagger$ is simply

$$a_{(1,1)}^\dagger = a^\dagger (a^\dagger a+1)^{-\frac{1}{2}} b^\dagger \,, \qquad (a^\dagger a = b^\dagger b) \,. \tag{44}$$

Hence the Hamiltonians (30) and (42) become

$$\hat{H}' \simeq a^{\dagger 2}\left[2(a^\dagger a+1)\right]^{-\frac{1}{2}} cd + \text{h.c.} \qquad (\text{PNA}) \,, \tag{45}$$

$$\hat{H}' = a^\dagger (a^\dagger a+1)^{-\frac{1}{2}} b^\dagger cd + \text{h.c.} \qquad (\text{PND}) \,. \tag{46}$$

As a crude approximation we substitute the intensity-dependent factors in Eqs. (45-46) with their constant average values and use the customary four wave mixing Hamiltonians

$$\hat{H}_{FWM} = a^{\dagger 2} cd + \text{h.c.} \qquad (\text{PNA}) \,, \tag{47}$$

$$\hat{H}_{FWM} = a^\dagger b^\dagger cd + \text{h.c.} \qquad (\text{PND}) \,. \tag{48}$$

In the parametric approximation of undepleted classical pump d, Eqs. (47-48) correspond to the interaction Hamiltonians

$$\hat{H}_I = a^{\dagger 2} c + \text{h.c.} \qquad (\text{PNA}) \,, \tag{49}$$

$$\hat{H}_I = a^\dagger b^\dagger c + \text{h.c.} \qquad (\text{PND}) \,. \tag{50}$$

The interaction time is rescaled by $\sqrt{I_d}$, I_d being the intensity of the pump d: the relation between the dimensionless time τ and the real time t (namely the length of the nonlinear medium) now reads

$$\tau = \chi^{(3)}\sqrt{I_d}t \,. \tag{51}$$

The Hamiltonians (47) and (48) were already suggested by Yuen[1], who inferred the amplifying performance from the conservation laws (23-24) and (37-38), with the assumption of complete conversion of the input signal. However, we will show that complete conversion is never achieved, apart from the case of one input photon. As an example in Fig. 1 the average output photon number is plotted for Hamiltonian (48) versus the interaction time τ, for both cases: number duplicator ($\langle n_a\rangle_0 = \langle n_b\rangle_0 = 0, \langle n_c\rangle_0 = n_i$) and number recombiner ($\langle n_a\rangle_0 = \langle n_b\rangle_0 = n_i, \langle n_c\rangle = 0$). An oscillatory quasiperiodic (or long-time periodic) behavior is evident, conversion never being complete at any time: the ideal gain is not reached, and the unconverted photons contribute to the output noise. Therefore, the saturating factors in Eqs. (45-46) are crucial to get complete conversion. Semiclassically a similar saturating behavior $\propto (1+I)^{-\frac{1}{2}}$ is obtained for interaction of radiation with a two level system in the inhomogeneously-broadening limit or in the adiabatic-following regime:[5] however, a full quantum treatment is still lacking and would require a wideband analysis. Here we only consider the performance of parametric Hamiltonians (49-50) in achieving approximate PNA and PND. In this case the interaction time $\tau = \tau_*$ for conversion depends on the input photon number n_i

$$n_i = \begin{cases} \langle n_c\rangle_0 \,, & (\langle n_a\rangle_0 = 0 \ : \text{direct operating mode}) \,, \\ \langle n_a\rangle_0 \,, & (\langle n_c\rangle_0 = 0 \ : \text{inverse mode}) \,, \end{cases} \tag{52}$$

which, in order to simulate the intensity-saturating low in Eqs. (45-46), should behave as follows

$$\tau_* \sim n_i^{-\frac{1}{2}} \,. \tag{53}$$

The conversion time (53) could be obtained tuning the pump intensity on the input photon number n_i: for n_i varying in a wide range, this would require a suited feedback mechanism based on a quantum nondemolition measurement of n_i. In the following we give more accurate evaluations of τ_*, using either analytical methods (a mean field approximation) and numerical calculations. The results obtained in the two ways will be compared and discussed in the end.

3.1 *A mean field approximation*

In Ref. [10] a linearization procedure for parametric conversion has been proposed, where Hamiltonians (49-50) are approximated in a selfconsistent way by the ideal ones (21) and (36). As we will see in the followings, this approach is correct only in the limit of large input photons numbers in the amplified/duplicated channels (i.e. a and b modes), namely it is suited to describe the inverse operating mode only. The method allows evaluation of the conversion time τ_*: its major limitation is that it leads to exact conversion and, therefore, there is no systematic way to estimate quantum fluctuations and nonideal gains. As a consequence, the direct operating mode cannot be described in terms of the time-reversed transformation of the inverse mode, because in this case knowledge of the output noise become essential. Therefore, in this section we analyze only the deamplifier/recombiner case.

The starting point of the method is to rewrite Hamiltonians (49-50) in a form similar to the ideal ones (21) and (36), namely

$$\hat{H}_I = f(a^\dagger a)Ac + A^\dagger f(a^\dagger a)c \,, \tag{54}$$

where

$$A = \begin{cases} a_{(2)} & (\mathrm{PNA}), \\ a_{(1,1)} & (\mathrm{PND}) \end{cases} \tag{55}$$

and

$$f(x) = \begin{cases} (2x+3-(-1)^x)^{\frac{1}{2}} & (\mathrm{PNA}), \\ (x+1)^{\frac{1}{2}} & (\mathrm{PND}). \end{cases} \tag{56}$$

The operator function $f(a^\dagger a)$ will be treated as a c-number time-dependent effective coupling, to be determined selfconsistently *a posteriori*. The Hamiltonian (54) is rewritten as

$$\hat{H}_I = f(a^\dagger a)Ac^\dagger + f(a^\dagger a - \nu)A^\dagger c\,, \tag{57}$$

where, in order to have a unified description of the two devices, the integer number ν is used

$$\nu = \begin{cases} 1 & (\mathrm{PNA}), \\ 2 & (\mathrm{PND}). \end{cases} \tag{58}$$

We write a mean field Hamiltonian taking the intermediate value $\bar{f}(a^\dagger a) = f(a^\dagger a - \frac{\nu}{2})$ between the two forms in Eq. (57) and averaging on the input state. One obtains

$$\hat{H}_{MF} = \bar{f}(n_a(\tau))\left[Ac^\dagger + \mathrm{h.c.}\right]\,, \tag{59}$$

where

$$n_a(\tau) = \langle a^\dagger(\tau)a(\tau)\rangle_0\,, \tag{60}$$

and

$$\bar{f}(x) = \sqrt{\nu\left(x+\frac{1}{2}\right)} \tag{61}$$

(the oscillating $(-1)^{n_a(\tau)}$ term in Eq. (56) is neglected). In the Dirac picture the time evolution of an operator $\hat{O}$ is written as follows

$$\hat{O}(\tau) \simeq \exp\left(i\hat{H}_{av}\tau\right)\hat{O}\exp\left(-i\hat{H}_{av}\tau\right)\,, \tag{62}$$

using the time-averaged Hamiltonian $\hat{H}_{av}$

$$\hat{H}_{av} = \frac{1}{\tau}\int_0^\tau \hat{H}_{MF}(\tau)d\tau = \frac{\theta(\tau)}{\tau}\left(Ac^\dagger + A^\dagger c\right)\,, \tag{63}$$

$$\theta(\tau) = \int_0^\tau \bar{f}(n_a(\tau'))d\tau'\,. \tag{64}$$

The evolution of the operators A and c takes the simple form

$$A(\tau) = A\cos\theta(\tau) + ic\sin\theta(\tau) \tag{65}$$

$$c(\tau) = c\cos\theta(\tau) + iA\sin\theta(\tau)\,. \tag{66}$$

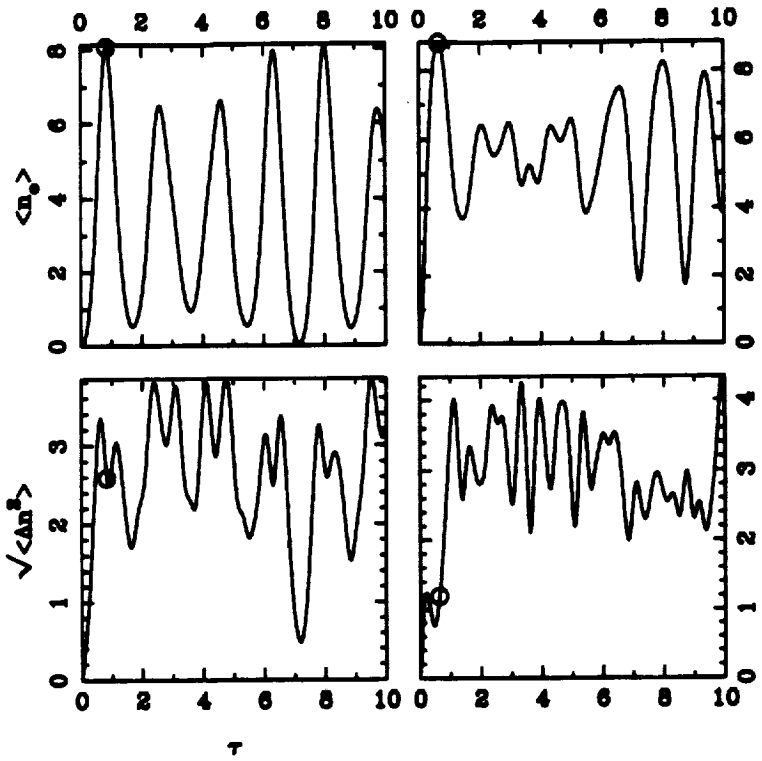

Figure 1: Time evolution of the output signal $\langle \hat{n}_o \rangle$ (figures on the top) and of the r.m.s. output noise $\sqrt{\langle \Delta \hat{n}^2 \rangle}$ (figures on the bottom) for parametric conversion (Hamiltonian (50)) of input number states with $n_i = 10$. The two figures on the left refer to the number duplicator ($\langle n_a \rangle_0 = \langle n_b \rangle_0 = 0, \langle n_c \rangle_0 = n_i$); those on the right to the number recombiner ($\langle n_a \rangle_0 = \langle n_b \rangle_0 = n_i, \langle n_c \rangle = 0$). The small circles enclose the conversion point corresponding to $\tau = \tau_*$.

We are now in a position to evaluate $n_a(\tau)$ selfconsistently. From Eq. (65) one has

$$n_A(\tau) = \langle A^\dagger(\tau) A(\tau) \rangle_0 = \langle A^\dagger A \rangle_0 \cos^2 \theta(\tau) \, . \tag{67}$$

For large input photons n_i and $\nu = 1$ the expectation n_A can be approximated as

$$n_A = [n_a/2] \simeq n_a/2 \, . \tag{68}$$

From Eqs. (64) and (67) we obtain the following integral equation for $n_a(\tau)$

$$n_a(\tau) = n_i \cos^2 \theta(\tau) = n_i \cos^2 \int_0^\tau \bar{f}(n_a(\tau')) d\tau' \, . \tag{69}$$

Differentiation of Eq. (69) leads to

$$\sqrt{\nu} d\tau = d\theta \left(n_i \cos^2 \theta + \frac{1}{2} \right)^{-\frac{1}{2}} \tag{70}$$

From Eqs. (65) and (69) one can see that complete conversion occurs at $\tau = \tau_*$ such that

$$\theta(\tau_*) = \frac{\pi}{2} \, . \tag{71}$$

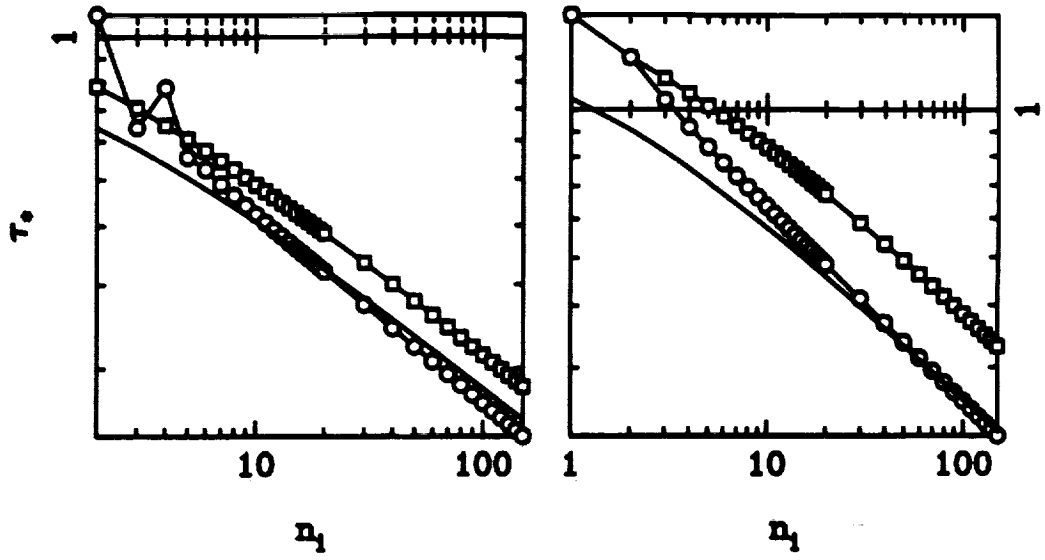

Figure 2: The best conversion time τ_* for parametric Hamiltonians (49-50) (PNA on the left and PND on the right). The squares are for the amplifier/duplicator, the circles for the deamplifier/recombiner. The lines without dots represent the mean-field approximation.

After integrating Eq. (70) from $\theta = 0$ to $\theta = \frac{\pi}{2}$ we find the conversion time as a function of the input photon number n_i

$$\tau_* = \nu^{-\frac{1}{2}} \left(n_i + \frac{1}{2}\right)^{-\frac{1}{2}} K\left(\frac{n_i}{n_i + \frac{1}{2}}\right) , \tag{72}$$

where $K(k)$ denotes the complete Jacobian elliptic integral

$$K(k) = \int_0^{\frac{\pi}{2}} (1 - k \sin^2 x)^{-\frac{1}{2}} dx . \tag{73}$$

For large numbers n_i, using the asymptotic behavior $K(k) \sim -\log \sqrt{1-k}$ for $k \to 1$, one obtains

$$\tau_* \sim \frac{1}{2} \nu^{-\frac{1}{2}} n^{-\frac{1}{2}} \log n , \tag{74}$$

which, a part from a logarithmic correction, has the same form of the preliminary result (53).

5. NUMERICAL RESULTS

The quantum evolution of input number eigenstates for the Hamiltonians (49-50) is evaluated numerically, taking advantage of the tridiagonal forms (28) and (40), which now read

$$\alpha_n^{(s)} = \sqrt{n(s - 2n + 1)(s - 2n + 2)} , \quad (s \equiv s_a) , \tag{75}$$

$$\beta_n^{(s)} = \sqrt{n}(s - n + 1) , \quad (s \equiv s_D) . \tag{76}$$

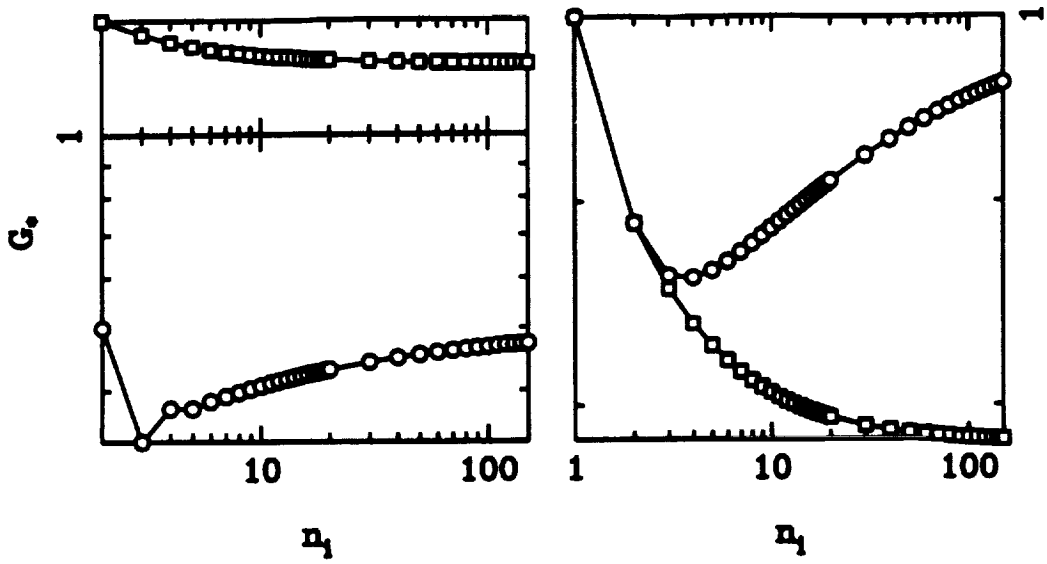

Figure 3: The maximum effective gain G_* (corresponding to the conversion time τ_* of Fig. 2) for parametric Hamiltonians (49-50) (PNA on the left, PND on the right). The squares are for amplification/duplication, the circles for the inverse operating mode.

The evolution of the output signal has been checked using the numerical results in Ref. [11]. In Fig. 1 we report a sample of the evolution for the PND. The time-dependence is periodic or nearly periodic for very low input photon numbers n_i, whereas it becomes more and more irregular (essentially irreversible) for increasing n_i. Qualitative differences between the direct and the inverse operating cases are evident. In the direct case the output signal exhibits maxima corresponding to high noise level, whereas low noise occurs only for depleted signal. In the inverse case, on the contrary, the first occurrence of a local maximum for the signal coincides with the absolute maximum, whereas the relative noise is always well below the subsequent values (this gap being an increasing function of n_i). The conversion is never complete in both cases, however, it is more efficient in the inverse operating mode, due to the low noise at the output. The conversion time τ_* has been identified as the time corresponding to the first local maximum of the signal (in the direct operating mode this could be slightly lower than the absolute maximum). The same features in the time evolution can be found for the PNA approximated by the conversion Hamiltonian (49), with analogous differences between the direct and inverse operating modes.

In Fig. 2 the conversion time τ_* is plotted against the input number n_i, for both Hamiltonians (49) and (50). The direct and inverse operating modes lead to two different curves, the former corresponding to longer conversion times τ_* (a part from some features which are peculiar of the deamplifier for low inputs n_i, and are reminiscent of the fractional behaviour (68)). The mean field approximation, which is pertinent only to the inverse operating mode, is reported for comparison. A good agreement is found for large n_i, better for the PND than for the PNA. For large n_i numerical best fits give power-low behaviours of the form $\tau_* \sim n^{-\alpha}$, with $\alpha \sim .4$ or smaller.

In Fig. 3 the maximum effective gain G_* (corresponding to the conversion time τ_* in Fig. 2) is reported. One can see that parametric conversion when used as a gain-two number amplifier

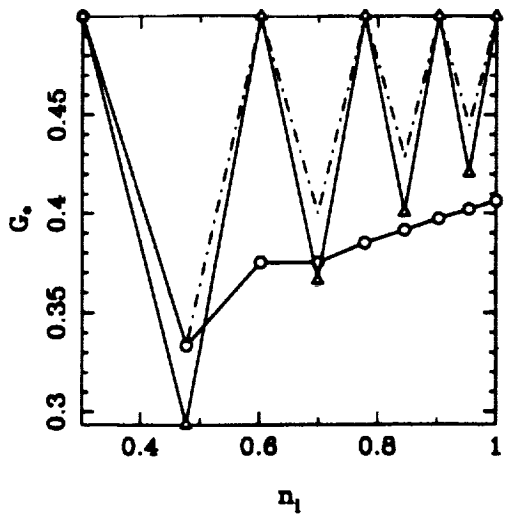

Figure 4: Effective gain G_* for the deamplifier with $G = 2$: circles and full line describe the parametric conversion (Hamiltonian (49)); triangles and full line describe the intensity-saturating Hamiltonian (45); dot-dashed line corresponds to the ideal deamplifier (5).

leads to an effective gain G_* which is a decreasing function of the input signal n_i, approaching the value $G_* \simeq 1.28$ for large n_i, well below the ideal gain. In a similar fashion the effective gain of the duplicator $G_* = \langle n_a(\tau_*)\rangle / \langle n_c(0)\rangle$ tends asymptotically to $G_* \simeq .78$. The inverse operating mode, on the contrary, behaves quite well, the deamplifier achieving the ideal $G_* = 1/2$ gain and the recombiner $G_* = 1$ in the large n_i limit. The deamplifier gain is compared with the ideal one (5) in Fig. 4, where also the intensity-saturating case (45) is reported [notice that in the direct operating mode the intensity-saturating Hamiltonians (45-46) lead to ideal behaviour].

Finally, in Fig. 5 the output Fano factors F_* at the conversion time τ_* are plotted. It is evident that parametric conversion lead to noisy PNA and PND, with $F_* \sim n^{-\beta}$ and exponent β slightly lower then 1: this corresponds to an output signal-to-noise ratio which is slowly (logarithmically) vanishing. The number deamplifier and recombiner are better approximated, with $F_* \simeq .13$ for large n_i: on the other hand, the intensity-saturating Hamiltonian (45) leads to vanishing F_* for large n_i (F_* is exactly zero for even n_i.)

6. CONCLUSIONS

We end with some remarks on physical interpretation of numerical results. We have seen that parametric Hamiltonians (45-46) are not good candidates for number amplification/duplication devices, whereas they could be profitably used to achieve approximate number deamplification/recombination. Here we emphasize that the source of noise in the simulated number devices is the socalled *spontaneous parametric emission*.[12] As a matter of fact, as explained in Ref. [11], the Hamiltonians (45-46) are formally similar to the Hamiltonian of a laser amplifier: in particular, Eq. (46) can be put in correspondence with the Hamiltonian describing a cluster of N two-level atoms

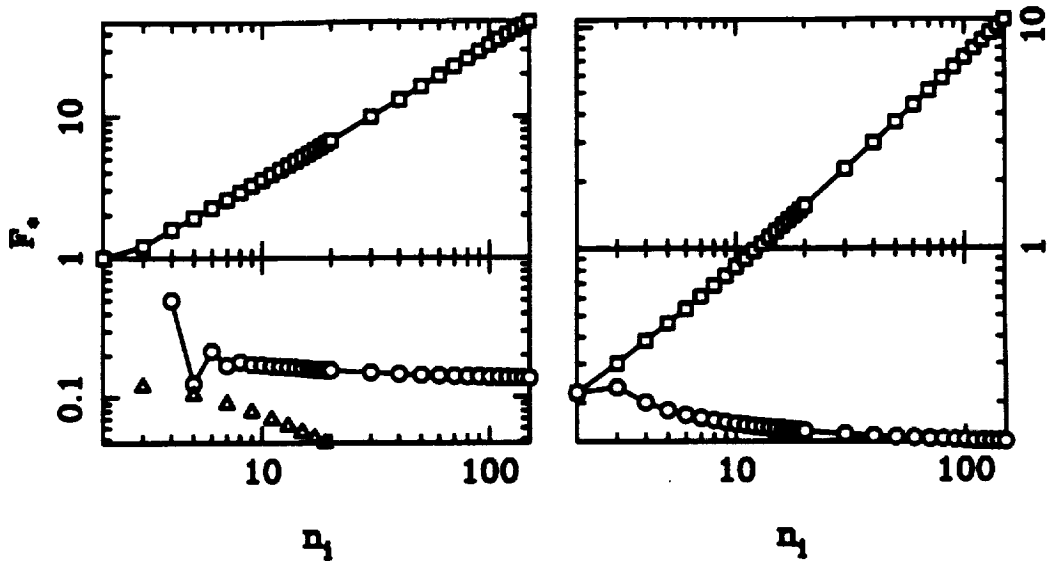

Figure 5: The Fano factor F_- at the conversion time τ_- of Fig. 2 for parametric Hamiltonians (49-50) (PNA on the left and PND on the right). The squares are for amplification/duplication, the circles for the inverse operating case. The triangles correspond to the intensity-saturating Hamiltonian (45).

interacting with one (resonant) mode of radiation

$$\hat{H}_I \propto a^\dagger \hat{J}_- + a \hat{J}_+ \,, \tag{77}$$

where $\hat{J}_\alpha = \sum_{i=1}^N \sigma_i^\alpha$ are the collective spin-flip operators for atoms. In fact, the angular momentum operators can be represented in terms of the two mode-operators b and c as follows

$$\begin{aligned} &\hat{J}_+ = bc^\dagger \,, \quad \hat{J}_- = b^\dagger c \,, \quad \hat{J}_z = \frac{1}{2}\left(c^\dagger c - b^\dagger b\right) \,, \\ &\hat{J} = \frac{1}{2}\left(c^\dagger c + b^\dagger b\right) \,, \quad J = \frac{N}{2} \,. \end{aligned} \tag{78}$$

When operating as a PND the Hamiltonian (46) acts on input states with $n_a = n_b$: in the direct operating mode one has $\langle n_a \rangle_0 = 0$ and $\langle n_c \rangle_0 = n_i$, whereas in the inverse $\langle n_a \rangle_0 = n_i$ and $\langle n_c \rangle_0 = 0$, namely $|M| = J$ in both case: this is exactly the spontaneous emission limit for the parametric converter (as opposed to the noisless coherent superradiant limit corresponding to $M = 0$). Thus, in conclusion, both the output noises and the nonideal effective gains are signs of the spontaneous parametric emission in the converter.

ACKNOWLEDGMENTS

We are grateful to R. Simonelli for numerical checks. This work has been supported by the *Ministero dell'Università e della Ricerca Scientifica e Tecnologica.*

REFERENCES

1 H. P. Yuen, in *Quantum Aspects of Optical Communications*, Ed. by C. Bendjaballah, O. Hirota, S. Reynaud, Lecture Notes in Physics **378** Springer, Berlin-New York, (1991), p.333

2 J. M. Shapiro and S. R. Shepard, Phys. Rev. A **43**, 3795 (1991)

3 G. M. D'Ariano, Int. J. Mod. Phys. B **6**, 1291 (1992) see also reference therein

4 G. M. D'Ariano, Phys. Rev. A **45**, 3224 (1992)

5 P. N. Butcher and D. Cotter, *The elements of nonlinear optics* (Cambridge University Press, Cambridge, 1991)

6 G. M. D'Ariano, C. Macchiavello, and M. Paris (unpublished)

7 S. L. Braunstein, Phys. Rev. A **42**, 474 (1990)

8 R. A. Brandt and O. W. Greenberg J. Math. Phys. **10** 1168 (1969)

9 G. M. D'Ariano, Phys. Rev. A **41**, 2636 (1990); Phys. Rev. A **43**, 2550 (1991)

10 J. Katriel and D. G. Hammer, J. Phys. A **14**, 1211 (1981)

11 D. F. Walls, in *Quantum Optics, Proceedings of the Scottish University Summer School, 10th; Edinburg 1969*, edited by S. M. Kay and Maitland (Academic, New York, 1970), p.501

12 R. Graham, in the same volume of Ref. [12], p.489